AMERICAN SOCIETY FOR MICROBIOLOGY | Applied and Environmental Microbiology®

ENVIRONMENTAL MICROBIOLOGY

DbdR, a New Member of the LysR Family of Transcriptional Regulators, Coordinately Controls Four Promoters in the *Thauera aromatica* AR-1 3,5-Dihydroxybenzoate Anaerobic Degradation Pathway

Daniel Pacheco-Sánchez,[a] Águeda Molina-Fuentes,[a] Patricia Marín,[a] Alberto Díaz-Romero,[a] Silvia Marqués[a]

[a]Consejo Superior de Investigaciones Científicas, Estación Experimental del Zaidín, Department of Environmental Protection, Granada, Spain

ABSTRACT The facultative anaerobe *Thauera aromatica* strain AR-1 uses 3,5-dihydroxybenzoate (3,5-DHB) as a sole carbon and energy source under anoxic conditions using an unusual oxidative strategy to overcome aromatic ring stability. A 25-kb gene cluster organized in four main operons encodes the anaerobic degradation pathway for this aromatic. The *dbdR* gene coding for a LysR-type transcriptional regulator (LTTR), which is present at the foremost end of the cluster, is required for anaerobic growth on 3,5-DHB and for the expression of the main pathway operons. A model structure of DbdR showed conserved key residues for effector binding with its closest relative TsaR for *p*-toluenesulfonate degradation. We found that DbdR controlled expression of three promoters upstream from the operons coding for the three main steps of the pathway. While one of them (P_{orf20}) was only active in the presence of 3,5-DHB, the other two (P_{dbhL} and P_{orf18}) showed moderate basal levels that were further induced in the presence of the pathway substrate, which needed be converted to hydroxyhydroquinone to activate transcription. Both basal and induced activities were strictly dependent on DbdR, which was also required for transcription from its own promoter. DbdR basal expression was moderately high and, unlike most LTTR, increased 2-fold in response to the presence of the effector. DbdR was found to be a tetramer in solution, producing a single retardation complex in binding assays with the three enzymatic promoters, consistent with its tetrameric structure. The three promoters had a conserved organization with a clear putative primary (regulatory) binding site and a putative secondary (activating) binding site positioned at the expected distances from the transcription start site. In contrast, two protein-DNA complexes were observed for the P_{dbdR} promoter, which also showed significant sequence divergence from those of the three other promoters. Taken together, our results show that a single LTTR coordinately controls expression of the entire 3,5-DHB anaerobic degradation pathway in *Thauera aromatica* AR-1, allowing a fast and optimized response to the presence of the aromatic.

IMPORTANCE *Thauera aromatica* AR-1 is a facultative anaerobe that is able to use 3,5-dihydroxybenzoat (3,5-DHB) as the sole carbon and energy source in a process that is dependent on nitrate respiration. We have shown that a single LysR-type regulator with unusual properties, DbdR, controls the expression of the pathway in response to the presence of the substrate; unlike other regulators of the family, DbdR does not repress but activates its own synthesis and is able to bind and activate three promoters directing the synthesis of the pathway enzymes. The promoter architecture is conserved among the three promoters but deviates from that of typical LTTR-dependent promoters. The substrate must be metabolized to an intermediate compound to activate transcription, which requires basal enzyme levels to always be present. The regulatory network present in this strain is designed to allow basal ex-

Citation Pacheco-Sánchez D, Molina-Fuentes Á, Marín P, Díaz-Romero A, Marqués S. 2019. DbdR, a new member of the LysR family of transcriptional regulators, coordinately controls four promoters in the *Thauera aromatica* AR-1 3,5-dihydroxybenzoate anaerobic degradation pathway. Appl Environ Microbiol 85:e02295-18. https://doi.org/10.1128/AEM.02295-18.

Editor Harold L. Drake, University of Bayreuth

Address correspondence to Silvia Marqués, silvia@eez.csic.es.

Received 19 September 2018
Accepted 24 October 2018
Accepted manuscript posted online 2 November 2018
Published 9 January 2019

pression of the enzymatic machinery, which would rapidly metabolize the substrate when exposed to it, thus rendering the effector molecule. Once activated, the regulator induces the synthesis of the entire pathway through a positive feedback, increasing expression from all the target promoters to allow maximum growth.

KEYWORDS α-resorcylate, LTTR, anaerobic biodegradation, denitrifiers, dihydroxylated aromatic, transcriptional regulation

The high production of aromatic compounds in the industrial world (1) and their deliberate or accidental release in the field have led to their accumulation in the environment (2). Bioremediation strategies for aromatic polluted sites are based on the ability of a number of microorganisms to efficiently metabolize these aromatic compounds, converting them into CO_2 and water. Bioremediation based on the activity of aerobic bacteria has been profusely used in the field, but polluted sites generally become anoxic once the oxygen present is consumed and depleted. Moreover, many polluted environments were anoxic from the start. Under these conditions, processes based on microorganisms capable of anaerobic metabolism are essential.

In the anaerobic degradation of aromatic compounds in bacteria, the activation of a broad range of compounds converges on a few major central metabolites, which are further dearomatized and channeled to the central cell metabolism (3–6). The most common of the central intermediates used by bacteria in the absence of oxygen is benzoyl coenzyme A (benzoyl-CoA), in which the carboxy-thioester group acts as an electron-withdrawing substituent that facilitates reduction of the aromatic ring (7). According to the respiratory metabolism of the host, this central intermediate is dearomatized by either an ATP-dependent (type I) or ATP-independent (type II) benzoyl-CoA reductase (8–10). In both cases, the resulting product, 1,5-dienoyl-CoA, undergoes further reduction and ring opening through a series of reactions similar to a modified β-oxidation (4). However, in several strains, benzoyl-CoA can also be formed under aerobic conditions from benzoate by a CoA ligase belonging to the so-called hybrid pathways (*box* genes), where it is then dearomatized by the activity of an oxygenase/reductase followed by ring cleavage through a dihydrodiol lyase (11).

An exception to the general pathway is the degradation of dihydroxylated aromatics in nitrate-reducing bacteria. The facultative denitrifying betaproteobacterium *Thauera aromatica* strain AR-1 attacks 3,5-dihydroxybenzoate (3,5-DHB; α-resorcylate) through an oxidative rather than a reductive reaction, where the aromatic ring is hydroxylated at position 2 by a water-dependent resorcinol hydroxylase (*dbhLS*) to render, after subsequent decarboxylation, the central intermediate hydroxyhydroquinone (HHQ) (12) (Fig. 1A). Similarly, in the strict anaerobe *Azoarcus anaerobius*, dihydroxybenzene (resorcinol) is converted to HHQ through hydroxylation of the aromatic ring at position 4 (13). These two strains were isolated from a sewage plant in Tubingen-Lustnau, Germany, for their capacity to grow on their corresponding aromatic substrates (14, 15). *Thauera aromatica* AR-1 can also grow anaerobically on benzoate through the classical benzoyl-CoA pathway (16), and anaerobic 3,4-dihydroxybenzoate degradation is also channeled through the benzoyl-CoA route (17). The strain is unable to degrade 3,5-DHB under strict aerobic conditions.

In *T. aromatica* AR-1, the 3,5-DHB-hydroxylating enzyme activity is membrane associated and produces the putative intermediate 2,3,5-trihydroxybenzoate as the primary product, which is then decarboxylated to HHQ. HHQ production is stimulated in the presence of an unidentified factor present in the cytoplasmic fraction (12). In both *T. aromatica* AR-1 and *A. anaerobius*, HHQ undergoes a nitrate respiration-dependent oxidation to 2-hydroxy-1,4-benzoquinone (HBQ), the first nonaromatic intermediate. The enzyme responsible for this step, HHQ dehydrogenase (benzenetriol dehydrogenase, encoded by *btdL*), is also membrane associated. HBQ is further metabolized to malate and acetate through a series of reactions starting with ring cleavage, probably through a multicomponent enzyme encoded by *bqdLMS* (18) (Fig. 1). The gene clusters coding for the enzymes of the pathway show a significant

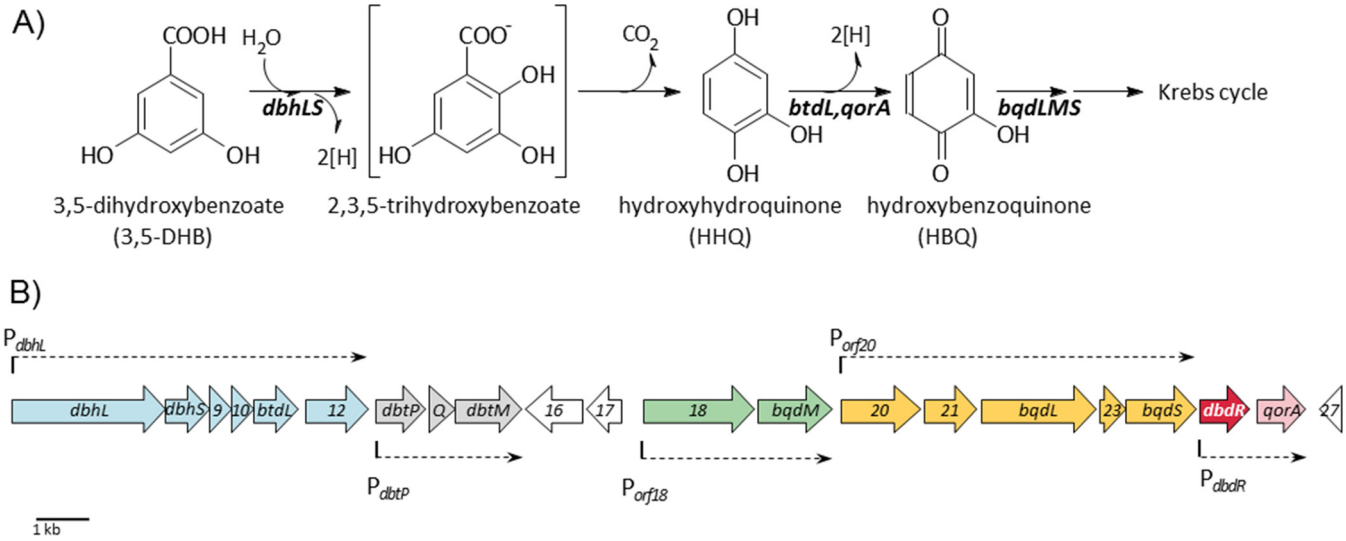

FIG 1 *T. aromatica* AR-1 3,5-DHB anaerobic degradation pathway and gene cluster. (A) *T. aromatica* strain AR-1 3,5-DHB degradation pathway. The genes involved in each enzymatic step are indicated. (B) Organization of the *T. aromatica* strain AR-1 genomic region coding for anaerobic 3,5-DHB degradation. The genes belonging to the same operon are shown in the same color, except the regulatory gene *dbdR*, which is shown in red. The promoters identified in this work are indicated, and the resulting transcripts as determined by reverse transcription-PCR (RT-PCR) (20) are outlined as dashed arrows. *dbhLS*, water-dependent hydroxylase; *btdL*, hydroxyhydroquinone dehydrogenase; *qorA*, quinone oxidoreductase; *bqdLMS*, hydroxybenzoquinone dehydrogenase; *dbtPQM*, TRAP transport system.

similarity between the two organisms, although with some differences (19, 20). In *T. aromatica* AR-1, the cluster is organized into four transcriptional units encoding the three main steps of the pathway and a tripartite ATP-independent periplasmic (TRAP) transport system. A fifth operon carries the *dbdR* gene coding for a LysR-type transcriptional regulator (LTTR) together with the *qorA* gene coding for a redundant enzyme for the second step of the pathway.

As is the case for the aerobic pathways, anaerobic aromatic degradation pathways appear to have recruited regulatory proteins belonging to diverse families to specifically control their expression in response to the presence of inducer molecules (21). The main enzymes of both dihydroxylated aromatic degradation pathways are induced by the presence of the substrate (16), which has been confirmed at the transcriptional level, both in *A. anaerobius* (22) and in *T. aromatica* AR-1 (20). Whereas the transcription in *A. anaerobius* of the three first pathway reactions is controlled by the coordinated activity of two homologous regulators belonging to the NtrC family (22), we have previously shown that in *T. aromatica* AR-1, the *dbdR* gene is required for growth in 3,5-DHB (20), suggesting that this LTTR is responsible for the expression of the different pathway operons.

The LTTR family is a highly conserved group of transcriptional regulators that are represented in all bacterial taxons and constitute the largest known family of prokaryotic DNA-binding proteins to date (23). Members of this family are composed of a highly conserved N-terminal winged helix-turn-helix (wHTH) DNA-binding domain (DBD) approximately 60 amino acids in length and an effector-binding domain (EBD) with lower sequence conservation but a conserved structural fold located in the C-terminal end of the protein (24). Both domains are connected by a long linker helix that confers the high flexibility required for the conformational changes that take place upon effector binding for promoter activation (24, 25). In recent years, the crystal structures of a significant number of family proteins have been determined, shedding some light on the transcription activation mechanism of this family. "Classical" LTTR-controlled systems consist of the regulator gene transcribed divergently from its regulated operon. The intergenic region includes a high-affinity binding site (primary binding site [PBS] [26], also known as the regulatory binding site [RBS]) that encompasses a T-N_{11}-A conserved region showing certain dyad symmetry and a generally

less-conserved secondary binding site (SBS; also known as the activating binding site [ABS]) partially overlapping the RNA polymerase −35 consensus sequence of the activated promoter. In many promoters, these two sequences show a certain degree of similarity (27). Once bound to the PBS and upon activation, e.g., through effector binding, the regulator undergoes a conformational change and establishes additional contacts with the SBS, which usually induces DNA bending, binding of the RNA polymerase, and transcription activation (24, 28). This physical organization leads to the regulator repressing its own synthesis while activating the target promoter. Whereas the PBS seems to be essential for LTTR binding, the SBS is essential for activation. In a number of regulators, a "sliding dimer" model of activation has been suggested. In these cases, additional binding sites are defined in the promoter region, and effector binding to the regulator provokes a conformational change that results in a shift of the DNA binding site, especially from a proximal SBS subsite to a distal SBS subsite, contributing to the relaxation of the DNA bending angle (29–31). In some other regulators, few changes in promoter binding are observed upon activation, and a mechanism differing from the sliding dimer is proposed (32). An increasing number of LTTR-regulated systems deviating from these architectures and activation mechanisms are being uncovered, so that no common activation mechanism can be proposed (33–37).

The main goal of this study was to characterize the transcriptional regulation controlling the growth of *T. aromatica* AR-1 on 3,5-DHB and the factors influencing pathway expression, among which the LTTR DbdR plays a pivotal role. Unlike most LTTRs, DbdR is not transcribed divergently from the genes it controls. Rather, it is able to simultaneously activate several promoters in the gene cluster, as well as its own expression. We were able to define four promoters of the pathway that were strictly dependent on this regulator, which responded to a pathway intermediate. An analysis of DbdR binding to its target promoters revealed differences in the binding modes to the promoters coding for pathway enzymes and to its own promoter.

RESULTS

Three promoters drive expression of the 3,5-DHB anaerobic degradation pathway in *T. aromatica* AR-1. To map the promoters driving transcription of the three main operons of the pathway, total RNA of *T. aromatica* AR-1 cells growing on either glutarate or 3,5-DHB was isolated and analyzed using primer extension with labeled oligonucleotides complementary to *dbhL*, *orf18*, and *orf20*. A single extension band was observed for *dbhL*, which only appeared when cells were grown on 3,5-DHB (Fig. 2A). The band size positioned the transcription start site 57 bp upstream from the translational start site of *dbhL*. Two extension bands were observed for *orf18* and *orf20*, which mapped 76 and 79 bp (P_{orf18}), and 70 and 71 bp (P_{orf20}) upstream from the translation start sites of *orf18* and *orf20*, respectively (Fig. 2B and C). The two P_{orf20} bands only appeared when 3,5-DHB was present, whereas the two P_{orf18} bands were present at low levels in glutarate-grown cells and were strongly induced in the presence of 3,5-DHB. These data confirm the inducibility of the pathway by the presence of substrate. An alignment of the sequences upstream from the transcription start sites showed a similar organization of the three promoters and several regions of high sequence conservation (Fig. 2D). The highest similarity was found between P_{dbhL} and P_{orf20}, with almost identical −10 and −35 boxes for RNA polymerase (RNAP) binding, identical sequences between positions −30 and −55 (coordinates relative to P_{dbhL} start site) that overlapped the −35 box, and a highly conserved (58% identity) region with partial symmetry between positions −57 and −75, which included the consensus LTTR binding motif T-N_{11}-A. Although less conserved, this motif was also present in P_{orf18}, as was the –30 to −55 conserved region which overlapped a significantly different −35 box. In P_{dbhL}, this sequence included a putative T-N_{11}-A binding motif which was not conserved in the two other promoters. The conservation of this motif might explain the higher activity levels obtained with this promoter (see below and Fig. 3). In all three promoters, the LTTR binding motif was centered at or near position −65 relative to

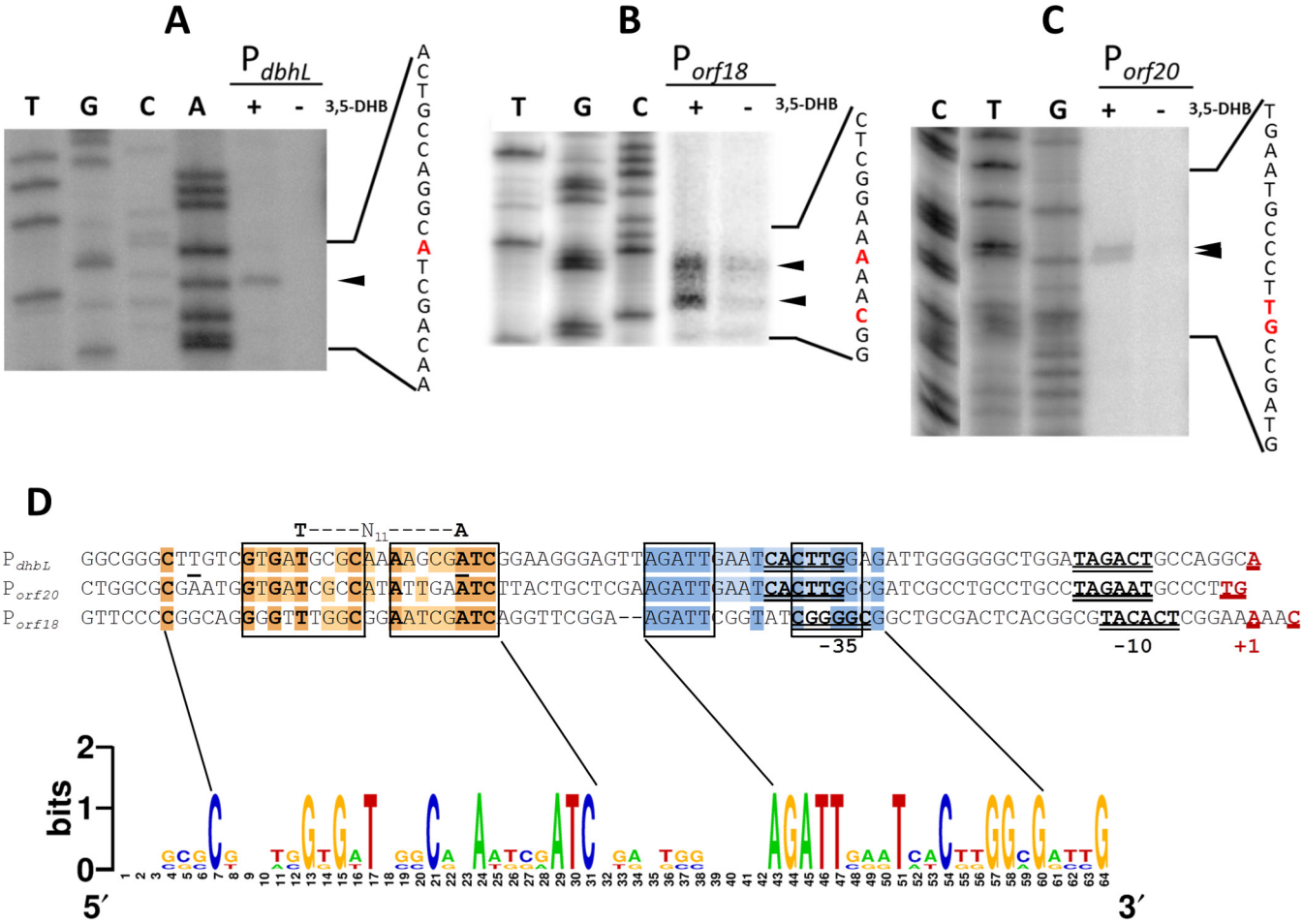

FIG 2 Mapping of the transcription initiation site of the three pathway operons. (A to C) Primer extension of total RNA of *T. aromatica* AR-1 cells growing on glutarate (−) or 3,5-DHB (+) with primers for P_{dbhL} (A), P_{orf18} (B), and P_{orf20} (C). The extension reactions were run parallel to sequencing reactions of the corresponding regions with the same primers. The cDNA extension bands corresponding to each promoter are indicated with arrowheads. (D) Alignment of the promoter regions of the three promoters showing the conserved RNA polymerase −10 and −35 binding elements (double underlined), the transcription start site (+1, red), and the conserved putative regulator binding sites located upstream (PBS, orange; SBS, blue; dark colored bases are conserved in the three promoters; light colored bases are conserved in two promoters). (E) Logo presentation of the conserved regions between the three promoters.

their transcription start sites, and corresponds to the so-called primary binding site (PBS) present in most LTTR-dependent promoters (28). We suggest that the conserved −30 to −55 region, placed 11 bp downstream from the T-N_{11}-A motif, would constitute the SBS site for promoter activation, as observed in other LTTR-dependent promoters (38, 39). However, we cannot rule out the binding of an additional, as yet unidentified, regulator(s) to this site.

DbdR controls expression of the pathway promoters. We have previously shown that the *dbdR* gene is essential for anaerobic growth on 3,5-DHB and is also required for the expression of the three main pathway operons (20). In fact, growth of a *dbdR* mutant on 3,5-DHB was restored when the *dbdR* gene was provided in a plasmid, as was the activity of the promoters (see Fig. S1 in the supplemental material). To confirm that the control of the three promoters was dependent on DbdR, we generated transcriptional fusions of the P_{dbhL}, P_{orf18}, and P_{orf20} promoters to *lacZ* in the pMP220 broad-host-range vector (40), and we transferred them to *T. aromatica* AR-1 and its *dbdR* null mutant (20). To allow normal growth of the mutant strain, the cells were cultivated on succinate in the presence and absence of 3,5-DHB, and β-galactosidase activity was determined after 72 h of growth. In the wild-type strain, P_{dbhL} and P_{orf18}, promoters of the first and second steps in the pathways and of one subunit of the third step, respectively, showed a significant basal activity in the absence of substrate, which

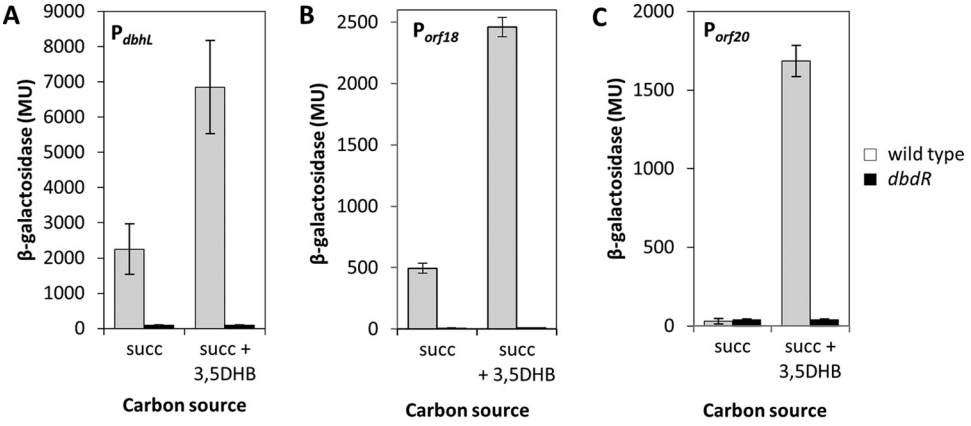

FIG 3 Expression of the three pathway promoters in wild-type and *dbdR* mutant backgrounds. β-Galactosidase activity was measured after 72 h in cultures of wild-type *T. aromatica* AR-1 and its *dbdR* mutant bearing the corresponding promoter-*lacZ* fusion in pMP220, growing on succinate or succinate plus 3,5-DHB. (A) P_{dbhL}; (B) P_{orf18}; (C) P_{orf20}.

was induced 3.5 and 5 times, respectively, in the presence of 3,5-DHB (Fig. 3). In contrast, the basal levels were negligible in P_{orf20}, and a strong induction was observed in the presence of 3,5-DHB. Both the basal and the induced activities of all three promoters were dependent on the presence of the *dbdR* gene. The unexpected differences between the two promoters with the highest sequence similarity, P_{dbhL} and P_{orf20}, especially in the absence of the effector, suggest that additional elements in the promoter sequence are relevant to determine the final promoter response and strength. Additionally, the T-N_{11}-A sequence included in P_{dbhL} suggested SBS might be relevant for the activity of this last promoter. In fact, it has been shown that minute changes in the DNA recognition elements or even in the flanking sequence can have drastic consequences on the affinity of the regulator for its binding site (41, 42).

The substrate must be transformed to activate DbdR. Although some LTTRs are capable of promoter activation in the absence of an effector, most of them require binding to a signal molecule to become active (28). This is especially true for those LTTRs regulating aromatic biodegradation pathways, which are generally recognized and activated by the substrate or by intermediate compounds in the degradation pathway (43). To test the interaction of DbdR with its substrate or with pathway intermediates, a His-tagged version of the protein was overproduced and purified using nickel-affinity chromatography, and the binding of possible effectors was tested using isothermal titration calorimetry (ITC). The assays were carried out under anoxic conditions, because the hydroxylated pathway intermediates become readily oxidized in the presence of oxygen. No binding signal was detected with 3,5-DHB and the first pathway intermediate hydroxyhydroquinone (data not shown). The first and third intermediates in the pathway, 2,3,5-trihydroxybenzoate and hydroxybenzoquinone, respectively, are not commercially available and could not be tested. We also tested two hydroxylated analogues as possible effectors of the protein; neither 2,5-dihydroxybenzoate (gentisate) nor 3,4-dihydroxybenzoate (protocatechuate) showed any interaction with the protein. As an alternative, we used a genetic approach to determine which intermediate of the pathway was essential for promoter activation *in vivo*. To that end, we measured promoter activity in genetic backgrounds unable to transform the substrate 3,5-DHB (a *dbhL* mutant), the third intermediate HHQ (a *btdL qorA* double mutant), and the fourth intermediate hydroxybenzoquinone (a *bqdL* mutant). Each of these mutants was expected to accumulate the corresponding substrate of the mutated enzyme gene. Fusions to *lacZ* of the three promoters were assayed in wild-type *T. aromatica* AR-1 and in its corresponding pathway mutants after 72 h of growth on glutarate in the presence and absence of 3,5-DHB. Figure 4 shows that in the *dbhL* mutant unable to transform 3,5-DHB, P_{dbhL} activity was similar in the absence and presence of the effector (i.e., basal

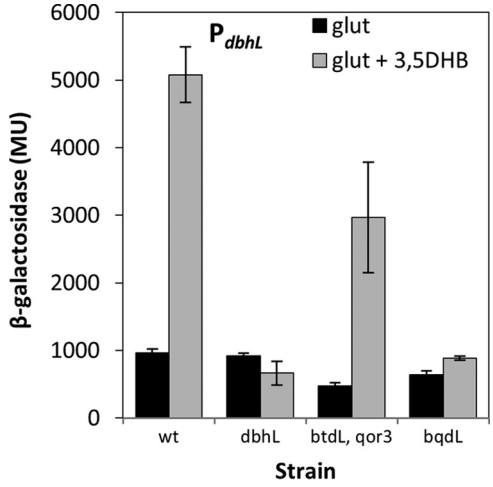

FIG 4 Identification of DbdR effector molecule. Data represent activity of P_{dbhL} in mutants of the first three pathway reaction steps. The β-galactosidase activity of wild-type (wt) *T. aromatica* AR-1 and the indicated knockout mutants bearing the P_{dbhL} promoter-*lacZ* fusion in pMP220 was measured after 72 h of growth on glutarate in the presence and absence of 3,5-DHB. Data are the averages from 3 to 4 assays. Results for P_{orf18} and P_{orf20} are shown in Fig. S2 in the supplemental material.

levels). The same was true for the *bqdL* mutant, where HBQ accumulated. However, in the *btdL qorA* double mutant, which lacks both pathways for HHQ transformation into HBQ and accumulates HHQ and probably its proposed precursor 2,3,5-trihydroxybenzoate, the activity of P_{dbhL} was significantly higher than in the two other mutants, reaching 60% of the wild-type values. A similar picture was obtained for P_{orf18} and P_{orf20}, where promoters were only induced by 3,5-DHB in the *btdL qorA* double mutant, reaching values of 92% and 57% of the wild type, respectively (see Fig. S2). These results point to HHQ or possibly 2,3,5-trihydroxybenzoate as the ligand required for the activation of DbdR to induce the three promoters.

DbdR is a tetramer in solution. In LTTRs, the effector binding domain (regulatory domain [RD]), is located at the C-terminal end of the protein. Its structure is composed of two Rossmann fold-like subdomains, leaving a cavity in the interface between them that constitutes the ligand binding site (also known as the inducer binding cavity) (29). Interestingly, the two closest DbdR homologues for which a crystal structure is available are the two LTTRs involved in the regulation of aromatic degradation pathways: *Comamonas testosteroni* strain T-S TsaR (30) and *Cupriavidus necator* CbnR (44), which control degradation of the aromatics *p*-toluenesulfonate and chlorocatechol, respectively. Figure 5 (top) shows the alignment of DbdR with TsaR and CbnR. As expected, the highest degree of sequence identity is located in the C-terminal domain (CTD), although homology is maintained throughout the whole protein sequence, especially in certain key residues involved in effector recognition (30). Figure 5 (bottom) shows the structure prediction of DbdR based on the crystal structure of TsaR, which locates DbdR DBD between residues 3 and 63 in the N-terminal domain (NTD), whereas the conserved EBD encompasses residues 87 to 297. A clear inducer binding cavity is identifiable between the two subdomains of the RD, which are well delimited in the structure. A long α-helix connects the DBD to the RD. In the TsaR protein, the residues putatively involved in *p*-toluenesulfonate binding have been identified (30). Similarly positioned residues are present in the DbdR binding cavity (Fig. 5; top): conserved Ser98 and Pro99 would face the side chain of the aromatic effector, whereas Pro199, 243, and 267 would create the hydrophobic environment accommodating the aromatic ring. These residues were also conserved in CatM and BenM proteins (45).

LTTRs are generally either dimers (33, 46) or tetramers (29, 47) in solution, although the majority of them are only active as DNA-bound tetramers (35). However, higher

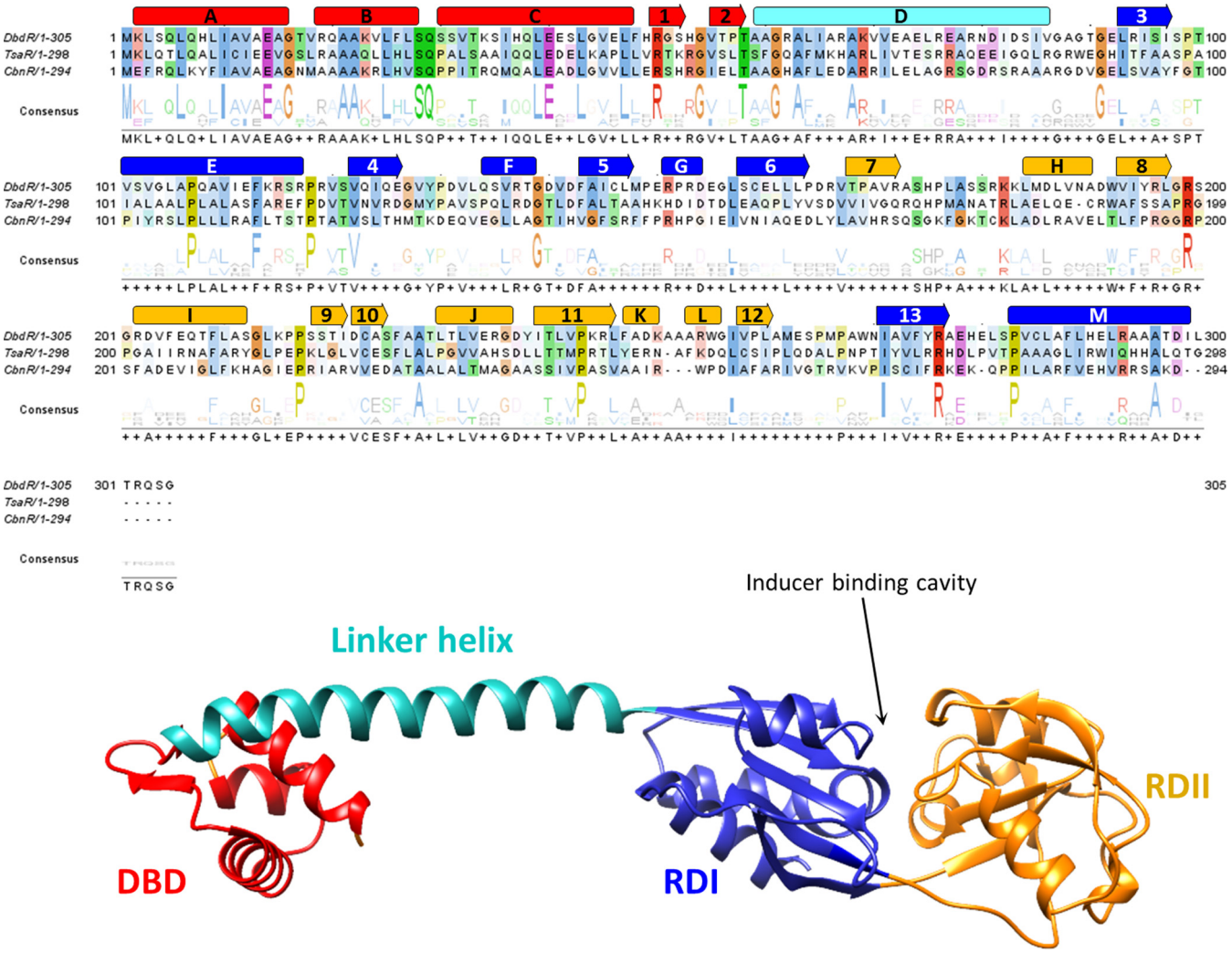

FIG 5 (Top) Alignment of *T. aromatica* AR-1 DbdR protein with its closest crystalized relatives TsaR (*Comamonas testosteroni*) and CnbR (*Cupriavidus necator*). The consensus sequence is presented as a Logo sequence. The sequence secondary structure predicted from the TsaR crystal is shown above the alignment as bars (α-helices) and arrows (β-strands), colored as at the bottom. (Bottom) Structure prediction of DbdR using the crystal structure of TsaR (c3fzjC) as a model (23). Helices and strands are colored as at the top to distinguish the domains and subdomains. DBD, DNA-binding domain, red; RD, regulatory domain composed of two subdomains, RDI (blue) and RDII (yellow); the linker helix is shown in turquoise.

level complexes (octamers) have also been suggested (48, 49). To determine the natural conformation of DbdR in solution, a His-tagged protein was overproduced in *Escherichia coli* and purified with nickel affinity chromatography. In SDS-PAGE analyses, the 6×His-DbdR monomers eluted with a molecular size of approximately 39.1 kDa, consistent with the sequence-deduced protein size (36.8 kDa). In analytical exclusion chromatography, purified DbdR eluted as a single peak corresponding to 161.8 kDa, suggesting that DbdR is a tetramer in solution (see Fig. S3).

DbdR binding to its target promoters. Initial electrophoresis mobility shift assays (EMSAs) of DNA fragments of the three promoters with His-tagged DbdR protein evidenced protein aggregation in the electrophoresis wells, impeding the penetration of the DNA fragment in the gel (not shown). The LTTRs are known to be poorly soluble, which hinders their purification and long-term storage (30). To avoid the purification steps that concentrate the proteins beyond manageable values, we performed EMSAs using purified extracts of an *E. coli* strain overproducing DbdR protein, as previously described for poorly soluble regulators (50). To that end, wild-type DbdR protein was expressed from a P_{lac} promoter in pBBdbdR in *E. coli* MC4100, and extracts of the cultures were obtained and passed through a heparin column to remove most unre-

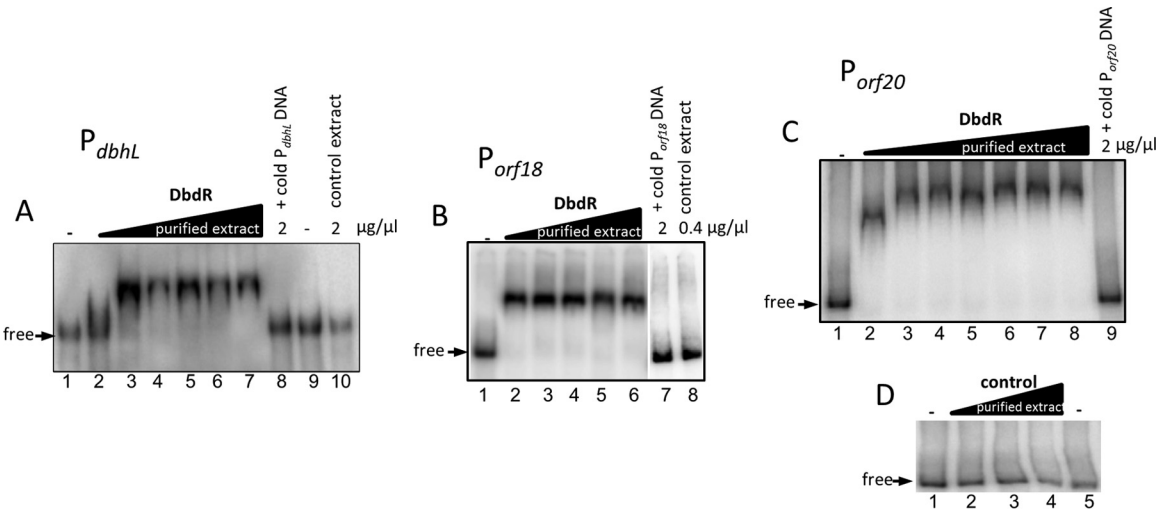

FIG 6 Binding of DbdR to P_{dbhL} (A), P_{orf18} (B) and P_{orf20} (C) promoter DNA. EMSAs of ^{32}P-labeled promoter DNA fragments with purified extracts containing DbdR protein were performed as described in Materials and Methods with either no protein added (lane 1) or increasing amounts of DbdR-enriched extract (purified extract): (A) 0.8, 1, 1.2, 1.6, 1.8, and 2 μg/μl; (B) 0.1, 0.2, 0.3, 0.4, and 0.8 μg/μl (lanes 2 to 6); (C) 0.5, 0.8, 1, 1.2, 1.6, 1.8, and 2 μg/μl (lanes 2 to 8). An excess of specific unlabeled promoter DNA fragment (lane 8 in panel A, lane 7 in panel B, and lane 9 in panel C) was added to a reaction mixture that also contained the maximum amount of crude extract. A purified extract lacking DbdR was used as a control at the indicated protein concentrations (panel A, lane 2; B, lane 8; D, lanes 2 to 5, protein range 0.8, 1.2, and 2 μg/μl).

lated DNA-binding proteins, which were eluted after applying 1 M NaCl (see Fig. S4). Bound and unbound fractions were tested with EMSAs for their ability to bind DNA fragments containing either of the three promoter regions spanning from more than 120 bp upstream from the transcription start site to more than 34 bp downstream (see Table 2). Only the heparin-unbound fraction (labeled "purified fraction") was able to form a specific and stable DNA-protein complex with the DbdR-dependent promoters, which appeared as a clearly shifted band in all cases (Fig. 6A to C). The presence of an excess of unlabeled competitor DNA titrated DbdR from its target DNA fragment (Fig. 6A, lane 8; Fig. 6B, lane 7; and Fig. 6C). To rule out the possibility of the extracts containing unrelated DNA-binding proteins capable of binding to these promoters, labeled promoter DNA fragments were incubated with increasing concentrations of similarly processed extracts from MC4100 cells carrying an empty pBBRMCS5 plasmid (control extracts). Those extracts lacking DbdR were incapable of producing DNA retardation with either promoter in EMSAs (Fig. 6A, lane10; Fig. 6B, lane 8; and Fig. 6D). In all cases, the DbdR-containing extracts only generated a single DNA-protein complex, consistent with DbdR being a tetramer in solution and binding its target promoter as such. Because DbdR is activated by the pathway intermediate HHQ, we repeated the assays in the presence and absence of this effector, although the anoxic conditions during incubation and electrophoresis could not be fully maintained. The presence of 1 mM HHQ in the binding assays resulted in a loss of retardation. However, this effect was not specific, and the addition of HHQ to unrelated binding assays with different regulators also resulted in a loss of interaction (data not shown), which we attributed to a toxic effect of HHQ on protein structure.

DbdR positively controls its own expression. In general, LTTRs also control their own expression through the interaction with the promoter of their gene, in most cases, located divergently from the pathway promoter they activate (28). In contrast, in *T. aromatica* AR-1, DbdR is transcribed downstream and in the same direction as the operon controlled by P_{orf20} (Fig. 1). We previously showed that *dbdR* is transcribed as a separate mRNA molecule that included the downstream *qorA* gene and independently of the operon controlled by P_{orf20} (20), which suggested the presence of a promoter directly upstream of the gene. We used primer extension assays to identify the promoter driving the expression of DbdR. Total RNA of *T. aromatica* AR-1 cells

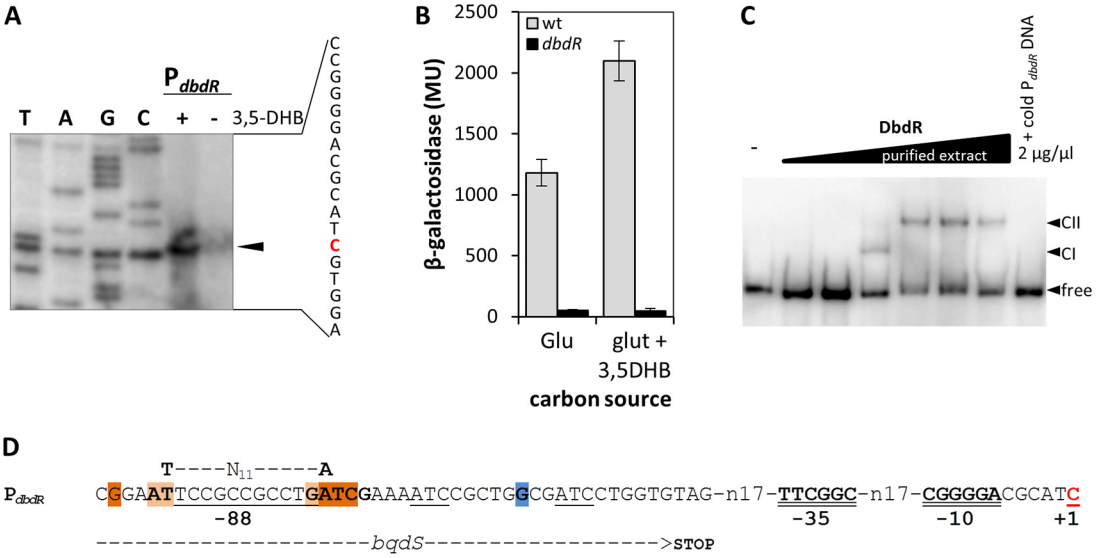

D

```
                T----N11-----A
PdbdR   CGGAATTCCGCCGCCTGATCGAAAATCCGCTGGCGATCCTGGTGTAG-n17-TTCGGC-n17-CGGGGACGCATC
                   -88                                      -35      -10      +1
        ---------------------bqdS------------------>STOP
```

FIG 7 Characterization of P_{dbdR} promoter. (A) Mapping of the transcription initiation site of P_{dbdR} as determined in primer extension of total RNA of *T. aromatica* AR-1 cells growing on glutarate (−) or 3,5-DHB (+) with a primer complementary to the *dbdR* gene. A sequencing reaction of the region with the same primer was run in parallel. (B) Expression of P_{dbdR} in wild-type and *dbdR* mutant backgrounds determined as β-galactosidase activity in 72-h cultures of wild-type *T. aromatica* AR-1 and its *dbdR* mutant bearing the corresponding promoter-*lacZ* fusion in pMP220, growing on glutarate or glutarate plus 3,5-DHB. (C) Binding of DbdR to P_{dbdR} promoter DNA: EMSA of ^{32}P-labeled promoter DNA fragment with increasing concentrations of purified extracts containing DbdR (0.025, 0.045, 0.075, 0.1, 0.8, and 1.2 μg/μl; lanes 2 to 7); −, no extract added (lane 1); lane 8, addition of specific unlabeled promoter DNA fragment to a reaction mixture that also contained the maximum amount of crude extract. A similar assay with control extracts lacking DbdR gave no retardation band (not shown). (D) P_{dbdR} promoter sequence showing the putative RNA polymerase binding (−10 and −35) and DbdR binding sequences. Bases conserved in the DbdR binding motifs of the remaining promoters are shown with the same color code as in Fig. 2. The position of the bases relative to the transcription start site (+1, red) is indicated below the sequence. The region spanning the end of *bqdS* gene is indicated.

growing on either glutarate or 3,5-DHB was isolated and analyzed with labeled oligonucleotides complementary to *dbdR*. A single extension band was observed that was more intense when cells were grown on 3,5-DHB. The band size positioned the transcription start site 36 bp upstream from the translational start site of *dbdR* and defined the RNAP binding site, which differed significantly from the previously defined consensus (Fig. 7D). Furthermore, the only putative DbdR binding site showing the conserved T-N_{11}-A sequence was detected centered at −88 bp from the transcription start site, which is unusually distant. It is worth noting that the intergenic region between the *dbdR* coding sequence and the preceding gene (*bqdS*) is 90 bp long, and only 53 bp separate the *dbdR* transcription start site and the *bqdS* stop codon (Fig. 7D). Thus, the DbdR binding site probably overlaps the *bqdS* sequence, which may explain the atypical location and sequence of the binding sites (Fig. 7D). Furthermore, a stem-loop structure was predicted 9 bp downstream from the *bqdS* stop codon that may constitute a transcription terminator (not shown).

A transcriptional fusion of P_{dbdR} to *lacZ* in pMP220 was assayed in a *T. aromatica* AR-1 wild-type strain and in a *dbdR* mutant, both in the presence and absence of substrate. Figure 7B shows that the promoter had high basal activity in the absence of substrate (approximately 1,200 MU), which increased almost 2-fold in the presence of 3,5-DHB. Both the basal and induced activities were strictly dependent on DbdR. Thus, unlike most LTTRs, DbdR is required to activate its own synthesis, which is further stimulated in the presence of an effector. Binding of DbdR to its own promoter was confirmed in an EMSA of a DNA fragment covering 312 bp upstream from the *dbdR* translation start site, with purified DbdR extracts prepared as described above (Fig. 7C). Interestingly, two retardation complexes were observed in this promoter, which we had never observed for the enzymatic operon promoters analyzed above at any protein concentration (Fig. 6 and not shown).

DISCUSSION

The anaerobic degradation pathway for 3,5-DHB in *T. aromatica* AR-1 involves oxidative rather than reductive steps as initial reactions for aromatic activation and metabolism, which depend on at least 20 genes organized in a 25-kb gene cluster. Efficient expression of the pathway requires the presence of the substrate in the medium and an intact copy of the regulatory gene *dbdR*, previously described as essential for anaerobic growth on the aromatic and for expression of some genes in the pathway (20). DbdR belongs to the LTTR family of regulators, which are generally transcribed divergently from the promoter they control. Actually, all LTTRs were initially believed to repress their own expression through binding at the same site required for activation of the divergent promoter (thus, originally called the repressor binding site [RBS]), which was especially true for many LTTRs regulating the aerobic degradation of aromatics (BenM, CatM, NahR, and TfdR, among others) (43). This is not the case for DbdR, which is transcribed downstream and independently of one of the operons under its control (20). In fact, the current view of LTTRs describes a more diverse organization of the genes than initially thought. In an increasing number of LTTR-controlled regulatory networks, the regulator is not divergently transcribed from its target promoter; some LTTRs can simultaneously control several target promoters, and in some cases, they also activate their own synthesis (33–37). We have shown that DbdR is capable of directly activating at least three promoters in the pathway which drive transcription of the enzymes essential for the initial reaction steps. The structure of the three promoters is conserved, with a clear LTTR box (PBS) centered approximately on position −65 and bearing the consensus GNGNTN$_3$CN$_2$AN$_4$ATC (underlined bases make up the palindromic T-N$_{11}$-A LTTR consensus). A putative SBS is found 11 bp downstream from the PBS (9 bp downstream in the case of P$_{orf18}$) and overlapping the −35 RNA polymerase binding site, bearing the consensus AGATTN$_3$TN$_2$CN$_2$GGNG that shows no obvious palindromic structure, as is the case for some SBS sites in LTTR-controlled promoters (28, 31). The functional organization of these sites is unknown, but its conservation in the three promoters is a clear indication of a pivotal role in promoter activation. The sequence similarity is especially remarkable between P$_{dbhL}$ and P$_{orf20}$, which control the transcription of the enzymes for initial 3,5-DHB activation and ensuing HHQ dearomatization and the cleavage of the nonaromatic product HBQ, respectively (Fig. 1). Despite the strong conservation between them (60% and 94% identity in the PBS and SBS sites, respectively) (Fig. 2D), their transcription patterns are different. P$_{dbhL}$ shows high basal DbdR-dependent expression levels, which are further increased in the presence of the substrate (Fig. 3A), whereas P$_{orf20}$ is completely inactive in the absence of substrate and becomes fully active when 3,5-DHB is present in the medium (Fig. 3C). Minute changes in the promoter sequence at positions within the regulatory elements have been shown to drastically influence promoter responsiveness to its LTTR by altering the affinity of the regulator for its promoter (41, 42). Although highly similar, the PBS and SBS sites of P$_{dbhL}$ and P$_{orf20}$ are not identical, and the few base pair differences between them may explain the lack of activation of P$_{orf20}$ by DbdR in the absence of an effector. For instance, P$_{dbhL}$ shows an A track within the PBS, which is absent in P$_{orf20}$ (Fig. 2D). A survey of LTTR-dependent promoters for the presence of A tracks in the binding sites shows that a not insignificant portion of them present A tracks within the SBS, and some of them show additional A or T tracks in the PBS, which were suggested to help the interaction of the regulator with their binding site(s) (51). Furthermore, P$_{dbhL}$ includes the T-N$_{11}$-A sequence in its putative SBS, which is absent in the other promoters. This may explain the high expression levels obtained by this promoter both in the presence and absence of an effector compared to that by P$_{orf20}$.

Using a genetic approach, we have shown that the pathway substrate 3,5-DHB must be metabolized to activate transcription from the three promoters. Our current knowledge of the pathway does not allow us to discern whether the accumulated intermediate in the *btdL qorA* double mutant responsible for DbdR activation is 2,3,5-

trihydroxybenzoate or HHQ. However, the conservation of the residues in the DbdR binding cavities with those of TsaR, CatM, and BenM, which respond to effectors bearing an acidic side chain, suggests that the unstable intermediate 2,3,5-trihydroxybenzoate might be the effector of DbdR. This would explain the absence of interaction of DbdR with HHQ in ITC assays. Regardless of the specific effector activating DbdR, this implies that in order for the pathway to become fully induced, the enzymatic machinery for the initial transformation of 3,5-DHB must already be available in the cell before uptake of the substrate. Our results suggest that the regulatory circuit is in fact designed to allow basal levels of 3,5-DHB hydroxylase (encoded by *dbhLS*) to be permanently present in the cell to transform the incoming substrate into an effector molecule. If the effector were actually HHQ, its fast production after exposure to 3,5-DHB would also be guaranteed. The transformation of the 2,3,5-trihydroxybenzoate produced by DbhLS into HHQ was shown to depend *in vitro* on an unknown protein factor present in the cytoplasmic fraction of *Thauera aromatica* AR-1 cell extracts (6, 12). The gene putatively responsible for this activity has not yet been identified, although *orf18*, which shows homology to a molybdopterin oxidoreductase, is a good candidate (20). Thus, both *dbhLS* and *orf18*, which we have shown to be significantly expressed even in the absence of substrate (Fig. 3), guarantee the transformation of 3,5-DHB into HHQ to activate the expression of the third pathway enzyme, HBQ dehydrogenase (*bqdLMS*) from P_{orf20}, which is essential for complete substrate degradation and anaerobic growth on this carbon source. We have previously shown that *Thauera aromatica* AR-1 growth on 3,5-DHB is significantly impaired in a mutant for the TRAP transport system encoded by *dbtPQM*, suggesting that this substrate needs to be transported into the cell by a dedicated machinery (20). We have located a promoter upstream from *dbtP* that showed high constitutive expression levels (D. Pacheco-Sánchez, unpublished), which would, if present, guarantee permanent substrate uptake into the cell (Fig. 1B).

LTTR proteins are known to be highly insoluble and difficult to obtain as concentrated protein solutions (52), essentially due to the poor solubility of their DNA binding domain (53). Our attempts to perform EMSAs with purified DbdR proved unsuccessful, because aggregates that did not enter the gel were observed with the different promoter DNAs. The use of DbdR-enriched fractions obtained from DbdR-overproducing *E. coli* extracts in our EMSAs circumvented the solubility problem. Using this approach, specific DbdR binding to the three promoter sequences was observed. Unfortunately, this method did not allow estimation of promoter affinity, since the actual DbdR concentration in the different extracts was not known. Based on our gel filtration data and on the structure of TsaR, the closest relative of DbdR crystalized so far, we predict that the DbdR native configuration is a tetramer, probably resulting from the association of two homodimers, which would be bound in an antiparallel configuration through their linker helix (24, 30). In the EMSAs of the three promoters, a single retardation band was always observed, suggesting that DbdR is actually binding these promoters directly as a tetramer (Fig. 6).

The situation is different for the P_{dbdR} promoter. Unlike most LTTRs, and especially unlike those transcribed divergently from their activated genes, DbdR was shown to activate transcription from its own promoter and to increase transcription 2-fold in the presence of the substrate (Fig. 7A and B). It is worth noting that *dbdR* is cotranscribed with the *qorA* gene, which encodes a quinone oxidoreductase required for efficient HHQ processing during 3,5-DHB degradation (20). Interestingly, the EMSA of the P_{dbdR} promoter with DbdR extracts showed the consecutive formation of two protein-DNA complexes, consistent with sequential binding of DbdR as dimers and further oligomerization to tetramers. Although gel filtration assays of purified DbdR protein indicated a tetrameric structure in solution, it is plausible that at the working protein concentrations in the purified extracts used in the EMSA, DbdR dimmers and tetramers coexist. The nitrogen assimilation control protein Nac of *Klebsiella pneumoniae* can activate transcription either as dimer or as tetramer, depending on the target promoter (33). In solution, the protein is a tetramer that dissociates into dimers when the protein

concentration decreases to a certain threshold (54). Interestingly, the activity of this LTTR is not controlled by an effector but rather is dependent on its concentration in the cell, which is regulated by NtrC. Thus, it is plausible that the P_{dbdR} promoter is occupied (and possibly activated) by DbdR at lower regulator concentrations, facilitating a positive feedback. The P_{dbdR} sequence shows no homology with the three promoters controlling the enzymatic genes, which probably results from the unusual location of the promoter overlapping the 3′ end of the upstream transcribed *bqdS* gene, and thus must adapt the sequence of the binding sites to the enzyme-coding sequence (Fig. 7D). We were able to identify a putative PBS around position −88, more than 20 bp further from the transcription start site than in the typical LTTR-dependent promoters. Furthermore, we were unable to predict any clear SBS in the sequence. It is conceivable that at P_{dbdR}, the different positioning of the binding sites implies a different DbdR promoter activation mechanism with a different protein rearrangement for activation, as described for other LTTRs targeting several promoters with a different operator organization (24, 33, 35). This can be seen as the regulator conformation and activation mechanism not only being controlled by the presence/absence of its effector but also being modulated by the specific operator sequence present at each promoter.

Overall, the results presented in this study show that a single LTTR coordinately controls expression of the entire 3,5-DHB anaerobic degradation pathway in *Thauera aromatica* AR-1. The regulator was essential for transcription of all the operons coding for the different enzymatic steps down to ring cleavage, as well as for transcription of its own gene. The regulatory network was such that it allowed basal expression of the enzymatic machinery required for the metabolism of the substrate to produce the effector molecule through the basal DbdR-dependent expression from P_{dbhL}. Once synthesized, the effector molecule induced the synthesis of the remaining pathway steps and initiated a positive feedback, increasing expression from all the target promoters to allow maximum growth. This included a 2-fold induction of its own promoter, which is not only important to maintain sufficient levels of the regulator to efficiently activate a previously silent fourth promoter (P_{orf20}) but also to synthesize the cotranscribed *qorA* gene required to efficiently remove HHQ, which, above a certain threshold, becomes toxic to the cell.

MATERIALS AND METHODS

Materials and standard procedures. All chemicals used in this study were from Fluka (Neu-Ulm, Germany), Sigma-Aldrich (Darmstadt, Germany), and Merck (Darmstadt, Germany). Restriction and other molecular biology enzymes were obtained from New England BioLabs (Ipswich, MA) and Roche (Basel, Switzerland). Plasmids were isolated with a QIAprep spin plasmid kit from Qiagen (Hilden, Germany). PCR products and cDNA were purified with a QIAquick gel extraction kit from Qiagen. Oligonucleotides were synthesized by Sigma-Aldrich. RNA was extracted using the TRI Reagent method (Ambion, Austin, TX). DNA sequencing was performed by the DNA Sequencing Service at the López-Neyra Parasitology and Biomedicine Institute (IPBLN, CSIC, Granada, Spain). Transformation, PCR amplification with the Expand high-fidelity system (Roche), and protein analysis were performed according to standard protocols (55).

Bacterial strains, plasmids, and culture conditions. The bacterial strains and plasmids used in this study are summarized in Table 1. *Thauera aromatica* strain AR-1 (15) bearing the 3,5-DHB-anaerobic degradation cluster (GenBank accession number KJ995609 [19]) and its mutant derivatives and transconjugants were grown anaerobically at 30°C without shaking in 50- or 100-ml infusion bottles containing nonreduced Widdel mineral medium under nitrogen gas prepared as described (20). The final medium (WMM) included 30 mM 3-(*N*-morpholino)propanesulfonic acid (MOPS) as buffer instead of bicarbonate and 8 mM potassium nitrate. The carbon sources used were stored in sterile infusion bottles under nitrogen gas and were added to the cultures with syringes to the final concentrations specified in "Growth experiments." For all genetic manipulations, *T. aromatica* strain AR-1 and derivatives were grown aerobically in WMM supplemented with glutarate 5 mM as the carbon source. Solid medium was prepared by adding 1.6% twice-washed Difco agar to the WMM medium. *Escherichia coli* strains HB101, DH5α, MC4100, and CC118λpir were grown aerobically at 37°C in Luria-Bertani (LB) medium. When appropriate, antibiotics were used at the following concentrations: tetracycline, 10 $\mu g \cdot ml^{-1}$; ampicillin, 100 $\mu g \cdot ml^{-1}$; kanamycin, 50 $\mu g \cdot ml^{-1}$, streptomycin, 50 $\mu g \cdot ml^{-1}$, and gentamicin, 10 $\mu g \cdot ml^{-1}$ (except for *T. aromatica* AR-1, for which tetracycline and kanamycin were used at 5 $\mu g \cdot ml^{-1}$ and 25 $\mu g \cdot ml^{-1}$, respectively).

Growth experiments. Infusion bottles (100 ml) containing 75 ml of anaerobic WMM were supplemented with the required antibiotics. The carbon source was one of the following: 3,5-DHB (1 mM), succinate (2 mM), glutarate (3.5 mM), or the combination of 3,5-DHB and succinate or 3,5-DHB and glutarate at the same concentrations as above. The bottles were inoculated with 1% of an exponentially

TABLE 1 Strains and plasmids used in this study

Strain or plasmid	Genotype/relevant characteristics[a]	Reference/ source
Strains		
Escherichia coli		
HB101	*supE44 hsdS20* (r_B^- m_B^-) *recA13 ara-14 proA2 lacY1 galK2 rpsL20* (Sm^r) *xyl-5 mtl-1*	59
CC118λpir	Δ(*ara-leu*)*araD* Δ*lacX74 galE galK phoA20 thi-1 rpsE rpoB argE recA1*, lysogenized with λpir	60
DH5α	*endA1 hsdR17 supE44 thi-1 recA1 gyrA* (Nal^r) *relA1* Δ(*argF-lac*) *U169 depR* φ80*dlac*Δ(*lacZ*)M15	61
MC4100	*AraD139* Δ(*argF-lac*) *U169 relA1 rpsL150* (Sm^r) *deoCL ptsF25 flbB5301 rbsR*	62
BL21(DE3)	F^- *ompT hsdSB* (r_B^- m_B^-) *gal dcm* λDE3	61
Thauera aromatica		
AR-1	Wild-type strain, degrades 3,5-DHB under denitrifying conditions (DSM-11528)	15
AR-1 *dbdR*	Km^r, *T. aromatica* AR-1 mutant strain with a disruption of dbdR gene	20
AR-1 *bqdL*	Km^r, *T. aromatica* AR-1 mutant strain with a disruption of bqdL gene	20
AR-1 Δ*btdL qorA*	Km^r, Gm^r, *T. aromatica* AR-1 mutant strain with a disruption of qorA gene and deletion in btdL gene	20
AR-1 *dbhL*	Km^r, *T. aromatica* AR-1 mutant strain with a disruption of dbhL gene	20
Plasmids		
pRK600	Cm^r; helper plasmid, oriColE1, mobRK2, traRK2	63
pMP220	Tc^r; broad-host-range promoter probe vector (lacZ)	40
pBBR1MCS-5	Broad-host-range, oriV RK2, Gm^r	64
pBBdbdR	965-kb PCR product containing dbdR gene inserted between HindIII and XbaI sites of pBBRMCS-5	This study
PCR2.1-TOPO	PCR product cloning vector, ori pUC, ori f1; Ap^r, Km^r	Invitrogen
pGEMT-T Easy	PCR product cloning vector, ori pUC, ori f1; Ap^r	Promega
p220Pdbhl	P_{dbhL}::*lacZ* in pMP220; Tc^r	This study
p220Porf18	P_{orf18}::*lacZ* in pMP220; Tc^r	This study
p220Porf20	P_{orf20}::*lacZ* in pMP220; Tc^r	This study
p220PdbdR	P_{dbdR}::*lacZ* in pMP220; Tc^r	This study
pET28b+	Expression vector for recombinant proteins with His_6 tag at the N terminus; Km^r	Novagen
pETDbdR	pET28b+ derivative containing dbdR gene; Km^r	This study

[a]Cm, chloramphenicol; Gm, gentamicin; Km, kanamycin; Tc, tetracycline.

growing culture of *T. aromatica* AR-1 or mutant derivatives and incubated anaerobically at 30°C. Samples were collected anoxically with a sterile syringe flushed with N_2 at different time points and used immediately for determination of the optical density at 600 nm (OD_{600}) or β-galactosidase activity.

Plasmid construction. Plasmids carrying transcriptional P_{dbhL}::*lacZ*, P_{orf18}::*lacZ*, P_{orf20}::*lacZ*, and P_{dbdR}::*lacZ* fusions were obtained as follows. DNA fragments containing the *dbhL* (328 bp), *orf18* (385 bp), *orf20* (345 bp), and *dbdR* (301 bp) promoter regions from *Thauera aromatica* AR-1 were amplified by PCR using the appropriate primers (Table 2) to generate flanking BglII (upstream) and XbaI (downstream) sites for the P_{dbhL} promoter, BglII (upstream and downstream) sites for the P_{dbdR} promoter, and BglII (upstream) and PstI (downstream) sites for the P_{orf18} and P_{orf20} promoters. These fragments were cloned in pGEM-T (Promega) or pCR2.1-TOPO (Invitrogen). The resulting plasmids carrying the promoters were digested

TABLE 2 Oligonucleotide primers used in this study

Primer	Sequence (5′→3′)[a]	Product (target plasmid)/purpose/size (bp)
BglIIpdbdr-F	AGATCTGTTCGCCGCGATCATCAACC	P_{dbdR} (p220PdbdR)/transcriptional fusion and EMSA/−263 to +34
BglIIpdbdr-R	AGATCTCTGGCAAATTCCCCGATTTCC	
BglIIpORF20-F	AGATCTGCGCAAGGCCCGCGAGC	P_{orf20} (p220Porf20)/transcriptional fusion/−122 to +72
PstIpORF20-R	CTGCAGCATGAATCGTCCTCGAAGAT	
BglIIpORF18-F	AGATCTGCCATGCCGGCAAGG	P_{orf18} (p220Porf18)/transcriptional fusion/−254 to +83
PstIpORF18-R	CTGCAGTCATCGCAACCCATCCTCC	
BglIIpdbhl-F	AGATCTGCGCAGCTCCGCAAC	P_{dbhL} (p220PdbhL)/transcriptional fusion and EMSA/−255 to +60
XbaIpdbhl-R	TCTAGACATAGTCCCCTCTGTATTGA	
NdeIDbdR-F	CATATGGTGGACGCGCATCGTGGATGATGCCG	*dbdR* (pETdbdR)/His-tagged protein purification/918
HindIIIDbdR-R	AAGCTTTATCAGCCGACTGACTGACG	
HindIIIDbdR-F	AAGCTTGTGGACGCGCATCGTGGATGATGCCG	*dbdR* (pBDbdR)/cleared extract preparation/918
XbaIDbdR-R	TCTAGAACCCGAGATCGAATTGCC	
EMSAORF18F	AGATCTTTGCTGCTGTGCGCCGGCAA	P_{orfi18}/EMSA/−254 to +83
PstIpORF18-R	CTGCAGTCATCGCAACCCATCCTCC	
EMSAORF20F	AGATCTTTGCTGCGCCGGCAAG	P_{orf20}/EMSA/−122 to +72
PstIpORF20-R	CTGCAGCATGAATCGTCCTCGAAGAT	
Priext-dbhL	TGTCGTCGAACTCGATCGGC	*dbhL*/primer extension
Priext-orf18	GCCCTCCAAAACAGCTTGATTC	*orf18*/primer extension
Priext-orf20	GGTCAATTCAAGGCCGGAGA	*orf20*/primer extension
Priext-dbdR	GCAGCTGGCTCAGCTTC	*dbdR*/primer extension

[a]Newly created restriction sites are underlined.

with the enzymes for the newly created flanking sites, and the promoter-containing fragment was cloned between the same sites of the broad-host-range promoter probe vector pMP220 (40) to create p220PdbhL, p220Porf18, p220Porf20, and p220PdbdR. The correct orientation of each promoter in pMP220 was confirmed by sequence analysis. For the construction of the plasmid pBBdbdR, the *dbdR* gene was amplified by PCR using the primers HindIIIDbdR-F and XbaIDbdR-R (Table 2) with genomic DNA from *T. aromatica* AR-1 as the template. The resulting product was purified and cloned in pGEM-T (Promega) and confirmed by sequence analysis. The pGEM-T derivatives were digested with HindIII/XbaI, and the fragment containing the *dbdR* gene was ligated in the same sites of pBBR1MCS-5 to create pBBdbdR. This plasmid was used for the complementation of the *dbdR* mutant.

Triparental conjugation. The promoter::*lacZ* fusion pMP220 derivatives were transferred to *T. aromatica* strain AR-1 (wild type) and its mutant derivatives AR-1 *dbdR*, AR-1 *bqdL*, AR-1 Δ*btdL* Δ*qorA*, and AR-1 *dbhL* obtained previously (20) by RP4-mediated mobilization. *T. aromatica* AR-1 was grown to saturation in WMM supplemented with glutarate (5 mM). The *E. coli* donor strain CC118λpir bearing the plasmids to be transferred and the *E. coli* HB101(pRK600) helper strain were grown overnight on LB medium in the presence of tetracycline and chloramphenicol, respectively. All steps were performed aerobically as follows: 1 ml of each *E. coli* culture and 15 ml of *T. aromatica* AR-1 culture were harvested by centrifugation (13,000 × g for 10 min at 10°C). Cell pellets were washed once with 1 ml of WMM. The three resulting cell pellets were combined in 100 μl WMM and distributed on a sterile 47-mm-diameter 0.22-μm-pore-size filter (Schleicher and Schuell, Germany) placed on an LB plate, and the plates were incubated overnight at 30°C. The filters were then transferred into 3 ml of WMM, and cells were washed off by vigorous vortexing. *T. aromatica* AR-1 transconjugants where selected by their resistance to tetracycline (pMP220::promotor) or kanamycin and tetracycline (*dbdR* mutant bearing plasmid pMP220::promotor) either anaerobically or aerobically in WMM supplemented with 5 mM glutarate to counterselect against *E. coli* donor and helper strains. The transconjugants were confirmed by PCR analysis. Complementation plasmids were transferred to *T. aromatica* AR-1 mutant strains as described above, except that *T. aromatica* AR-1 mutant transconjugants were selected aerobically for their resistance to gentamicin in WMM supplemented with 5 mM glutarate.

β-Galactosidase assays. For assays in *T. aromatica* AR-1 and its mutants, 3-ml volumes of WMM supplemented with 5 mM glutarate as the carbon source and the required antibiotics were amended with a single colony of each strain bearing the appropriate combination of plasmids and incubated aerobically (100 rpm) for 3 days at 30°C as described above. This pregrown culture was used to inoculate 45 ml of WMM supplemented with the appropriate carbon source, which was grown for 3 days under anoxic conditions as described above, and constituted the anoxic inoculum. Finally, this preculture was used to inoculate the anoxic cultures to be assayed to an initial OD of 0.05 in serum bottles containing 45 ml of WMM supplemented with the appropriate carbon source and antibiotics. These cultures were incubated under anoxic conditions at 30°C without shaking. At the times indicated in the legends to Fig. 3, 4, and 7, 1 ml culture was collected by centrifugation, and β-galactosidase activity was determined in permeabilized whole cells according to Miller (56). Assays were minimally performed in triplicates, and standard errors of the means were calculated.

RNA preparation. *T. aromatica* AR-1 was grown at 30°C under nitrate-reducing conditions with 1 mM 3,5-DHB and/or 3.5 mM glutarate as the carbon source. Cells (45 ml) were harvested by centrifugation (8,000 × *g* for 5 min at 4°C) in disposable plastic tubes precooled in liquid nitrogen, and the pellets were kept at −80°C until use. RNA was extracted using the TRI Reagent method (Ambion, Austin, TX) with the following modifications (57): the lysis step was carried out at 60°C, and a final digestion step with RNase-free DNase was added at the end of the process. The RNA concentration was determined with a NanoDrop (Thermo Scientific), and RNA integrity was assessed by agarose gel electrophoresis.

Primer extension analysis. Oligonucleotides complementary to the coding strand of the *dbhL*, *orf18*, *orf20,* and *dbdR* genes (Table 2) were ^{32}P labeled at their 5′ ends in a 10-μl final volume that contained 1 μl 10× T4 polynucleotide kinase buffer (Roche), 10 pmol oligonucleotide, 1 μl [γ-^{32}P]ATP (6,000 mCi/mmol), and 1 U phage T4 polynucleotide kinase (Roche). The reaction mixtures were incubated for 1 h at 37°C and 10 min at 70°C to inactivate the kinase, and the labeled oligonucleotide was filtered through a Micro Bio-Spin column (Bio-Rad) to eliminate unbound nucleotide. Labeled primers were annealed to total RNA isolated as described above in 10 μl annealing mixture that contained 2 μl 5× annealing buffer {2 M NaC1, 50 mM PIPES [piperazine-*N*,*N*-bis(2-ethanesulfonic acid)], pH 7.0}, 10^5 cpm of 5′-end-labeled primer, and 10 to 30 μg total RNA template. The mixtures were first heated at 95°C for 3 min, incubated at 65°C for 5 min, and then slowly cooled to 44°C. cDNA was synthesized by the addition of 40 μl of reverse transcriptase buffer to bring final concentrations to 50 mM Tris-HCl (pH 8.5), 1 mM dithiothreitol (DTT), 8 mM $MgCl_2$, 30 mM KCl, 1 mM (each) all four deoxynucleoside triphosphates (dNTPs), 0.4 U/μl of RNase inhibitor (Roche), and 8 U avian myeloblastosis virus (AMV) reverse transcriptase (Roche). The mixtures were incubated for 1 h at 44°C, and the reaction was halted by the addition of 5 μl 3 M sodium acetate and 150 μl ethanol. The products of reverse transcription were analyzed in urea-polyacrylamide sequencing gels. Gels were exposed to a Molecular Imager model GS-525 (Bio-Rad). The DNA sequence was patterned using the DNA Cycle Sequencing kit based on the Sanger method (dideoxy chain termination method) according to the manufacturer's instructions, except that ^{32}P-labeled primers (1 μl, 6.5 × 10^5 cpm) were used instead of fluorescence-labeled primers.

Overproduction and purification of His-tagged DbdR by affinity chromatography. The *dbdR* gene was amplified by PCR using the primers NdeIDbdR-F and HindIIIDbdR-R (Table 2). The resulting products was purified and cloned into pGEM-T (Promega), which was then sequenced to rule out the presence of mutations. The pGEM-T derivative was digested with NdeI/HindIII, and the fragment containing the *dbdR* gene was ligated and fused in frame to pET28b+ to create pETDbdR. *E. coli* BL21(D3)

transformed with plasmid pETDbdR was used to overproduce the protein with the His tag. The cells were grown in 1 liter of 2× yeast extract-tryptone (YT) medium supplemented with 25 μg/ml kanamycin in an Erlenmeyer flask on a rotary shaker at 37°C. When the cells reached an A_{660} of 0.6, protein expression was induced with 0.1 mM IPTG (isopropyl-β-D-thiogalactopyranoside), and the incubation was continued for 20 h at 18°C. The cells were then harvested and stored at −20°C until use. Frozen cells were suspended in 25 ml of buffer A (20 mM Tris-HCl [pH 7.9], 500 mM NaCl, 10% glycerol, 1 mM DTT, and 10 mM imidazole) and lysed by 3 passages through a French pressure cell. The crude extract was centrifuged at 13,000 × *g* for 1 h at 4°C. The supernatant was passed through a 0.45-μm-pore-size filter and loaded onto a 5-ml Ni-agarose column (Amersham Biosciences) preequilibrated with buffer A in an ÄKTA (GE Healthcare) fast protein liquid chromatography (FPLC) system. Nonspecifically bound material was washed with six volumes of the same buffer plus 10 mM imidazole, and then a linear gradient from 20 mM to 500 mM imidazole in buffer B (20 mM Tris-HCl [pH 7.9], 500 mM NaCl, 10% glycerol, 1 mM DTT) was applied at a flow rate of 1 ml · min^{-1} for 30 min. Fractions of 2 ml were harvested; the 6×His-DbdR protein eluted between 150 mM and 250 mM imidazole. The purity of the 6×His-DbdR protein was analyzed by 12.5% SDS-PAGE. The protein was dialyzed overnight against buffer B and quantified via Bradford assay (Bio-Rad), and aliquot fractions were stored at 4°C.

Analytical size exclusion chromatography. The native molecular mass of purified 6×His-DbdR protein was determined by gel filtration chromatography using an FPLC Superdex 200 HR 10/30 (GE Healthcare) column. The buffer used for the gel filtration chromatography was the working buffer used for the purification of 6×His-DbdR (see above) without imidazole and DTT. Approximately 0.45 mg of purified 6×His-DbdR protein was applied at a flow rate of 0.5 ml · min^{-1}. The molecular mass of DbdR was estimated from a plot of the elution volume against the logarithm of the molecular masses of the following protein standards (Sigma): β-amylase, 4 mg/ml (200 kDa); alcohol dehydrogenase, 5 mg/ml (150 kDa); albumin, 10 mg/ml (66 kDa); carbonic anhydrase, 3 mg/ml (29 kDa); and cytochrome *c* (C7150), 2 mg/ml (12.4 kDa). Blue dextran (2 mg/ml, 2,000 kDa) was used to calculate the void volume.

Preparation of cleared-out extracts enriched in DbdR. *E. coli* MC4100 bearing pBBdbdR was grown overnight in LB with streptomycin and gentamicin at 30°C and 200 rpm. Flasks containing 500 ml of fresh medium were inoculated with an aliquot of these precultures and incubated at 30°C until an OD_{660} of 0.6 was reached, when they were induced with 1 mM IPTG and incubation was continued for 20 h at 30°C. The cells were then harvested by centrifugation, and the cell pellets were stored at −80°C until use. Crude extracts were prepared by suspending the pellet in 5 ml lysis buffer (20 mM Tris-HCl [pH 7.9], 500 mM NaCl, 1 mM DTT, and 1× Complete protease inhibitor mixture [Roche Applied Science]) followed by cell disruption by sonication. The clear supernatant was filtered through a 0.45-μm-pore-size nylon membrane and loaded onto a 1-ml heparin column (HiTrap heparin HP; Amersham Biosciences) preequilibrated with buffer C (Tris-HCl, 20 mM [pH 7.6]; DTT, 1 mM). Unbound proteins, which included DbdR, were collected and labeled "purified extract." The column was then washed with buffer C until nonspecifically bound material had been removed. Specifically bound proteins were eluted from the column with buffer C supplemented with 1 M NaCl, collected, and labeled "bound extract." The protein concentration in the fractions was determined according to Qubit assays. DbdR-free control extracts were obtained with a similar procedure but starting from *E. coli* MC4100(pBBR1MCS-5) cultures.

Electrophoretic mobility shift assays. The promoter regions of P_{dbhL}, $P_{orf18'}$ $P_{orf20'}$ and P_{dbdR} were amplified by PCR using *T. aromatica* AR-1 chromosomal DNA as the template and the primer pairs indicated in Table 2. These were then cloned into pCR2.1-TOPO (Invitrogen) or pGEM-T (Promega), rendering plasmids pGEMT::dbhL, pGEMT::orf18, pGEMT::orf20, and pTOPO::dbdR, respectively. The plasmids were sequenced to ensure the absence of mutations, and the promoter fragments for ^{32}P end-labeling either were obtained by PCR with the primers shown in Table 2 for P_{orf18} and P_{orf20} or were obtained after plasmid restriction with the appropriate enzymes for P_{dbhL} and P_{dbdR}. After electrophoresis, the fragments (ranging from 205 to 350 bp, approximately) were isolated from agarose gels and end labeled with [γ-^{32}P]ATP using T4 polynucleotide kinase. A concentration of 2 nM end-labeled DNA fragment (1.5 × 10^4 cpm) and the amounts of DbdR-enriched cell extracts indicated in the figure legends were mixed and incubated at 30°C for 15 min in 10 μl of binding buffer (50 mM Tris-HCl [pH 7.8], 50 mM KCl, 100 mM NaCl, 8 mM magnesium acetate, 5% [wt/vol] glycerol) containing 20 μg/ml of poly(dI-dC) as competitor DNA and 200 μg/ml bovine serum albumin. The DNA-protein complexes were resolved by electrophoresis in 4% (wt/vol) nondenaturing polyacrylamide gels and electrophoresed at 50 V in Tris-glycine buffer for 2 h at room temperature. The gels were dried and visualized by exposure to Phosphorimager screens. The results were analyzed with Molecular Imager FX equipment and Quantity One software (Bio-Rad).

Isothermal titration calorimetry. Titrations of 6×His-tagged DbdR were carried out in a VP microcalorimeter (MicroCal, Northampton, MA) at 25°C under anoxic conditions, because the hydroxylated pathway intermediates are highly sensitive to oxygen. Before starting, proteins were dialyzed against oxygen-free buffer B obtained by flushing nitrogen gas through the solution for 20 min. The 6×His-DbdR protein was placed in the sample cell of the instrument previously flushed with dinitrogen. The ligands were prepared in the degassed dialysis buffer. The ligands used were 3,5-DHB, hydroxyhydroquinone, and the hydroxylated analogues gentisate and benzoquinone (Sigma-Aldrich). Control experiments entailed the titration of dialysis buffer with ligand solutions.

Protein modeling. The tridimensional models of DbdR protein structure were generated with the Phyre2 tool available at http://www.sbg.bio.ic.ac.uk (58). The proteins used as models were obtained from the Protein Data Bank on the www.rcsb.org server: TsaR (c3fzjC) and CbnR (c1iz1B). Using TsaR as a template, Phyre2 modeled the structure of DbdR with 100.0% confidence and 96% sequence coverage.

SUPPLEMENTAL MATERIAL

Supplemental material for this article may be found at https://doi.org/10.1128/AEM.02295-18.

SUPPLEMENTAL FILE 1, PDF file, 0.2 MB.

ACKNOWLEDGMENTS

This work was supported by FEDER and grants from the Spanish Ministry of Science and Technology (BIO2011-23615) and Ministry of Economy and Competitiveness (BIO2014-54361-R). Á. Molina-Fuentes was the recipient of an I3P contract from the European Social Funds.

We thank Evaristo Manrique Roldán and Pablo Gómez Martín for their help with β-galactosidase activity determination and Angela Tate for improving the English language in the manuscript.

REFERENCES

1. Han D, Currell MJ. 2017. Persistent organic pollutants in China's surface water systems. Sci Total Environ 580:602–625. https://doi.org/10.1016/j.scitotenv.2016.12.007.
2. Breivik K, Armitage JM, Wania F, Sweetman AJ, Jones KC. 2016. Tracking the global distribution of persistent organic pollutants accounting for e-waste exports to developing regions. Environ Sci Technol 50:798–805. https://doi.org/10.1021/acs.est.5b04226.
3. Foght J. 2008. Anaerobic biodegradation of aromatic hydrocarbons: pathways and prospects. J Mol Microbiol Biotechnol 15:93–120. https://doi.org/10.1159/000121324.
4. Heider J. 2007. Adding handles to unhandy substrates: anaerobic hydrocarbon activation mechanisms. Curr Opin Chem Biol 11:188–194. https://doi.org/10.1016/j.cbpa.2007.02.027.
5. Heider J, Fuchs G. 1997. Anaerobic metabolism of aromatic compounds. Eur J Biochem 243:577–596. https://doi.org/10.1111/j.1432-1033.1997.00577.x.
6. Schink B, Philipp B, Muller J. 2000. Anaerobic degradation of phenolic compounds. Naturwissenschaften 87:12–23. https://doi.org/10.1007/s001140050002.
7. Fuchs G, Boll M, Heider J. 2011. Microbial degradation of aromatic compounds - from one strategy to four. Nat Rev Microbiol 9:803–816. https://doi.org/10.1038/nrmicro2652.
8. Boll M, Loffler C, Morris BE, Kung JW. 2014. Anaerobic degradation of homocyclic aromatic compounds via arylcarboxyl-coenzyme A esters: organisms, strategies and key enzymes. Environ Microbiol 16:612–627. https://doi.org/10.1111/1462-2920.12328.
9. Buckel W, Thauer RK. 2013. Energy conservation via electron bifurcating ferredoxin reduction and proton/Na(+) translocating ferredoxin oxidation. Biochim Biophys Acta 1827:94–113. https://doi.org/10.1016/j.bbabio.2012.07.002.
10. Kung JW, Baumann S, von Bergen M, MüLler M, Hagedoorn P-L, Hagen WR, Boll M. 2010. Reversible biological Birch reduction at an extremely low redox potential. J Am Chem Soc 132:9850–9856. https://doi.org/10.1021/ja103448u.
11. Gescher J, Eisenreich W, Worth J, Bacher A, Fuchs G. 2005. Aerobic benzoyl-CoA catabolic pathway in *Azoarcus evansii:* studies on the non-oxygenolytic ring cleavage enzyme. Mol Microbiol 56:1586–1600. https://doi.org/10.1111/j.1365-2958.2005.04637.x.
12. Gallus C, Schink B. 1998. Anaerobic degradation of α-resorcylate by *Thauera aromatica* strain AR-1 proceeds via oxidation and decarboxylation to hydroxyhydroquinone. Arch Microbiol 169:333–338. https://doi.org/10.1007/s002030050579.
13. Philipp B, Schink B. 1998. Evidence of two oxidative reaction steps initiating anaerobic degradation of resorcinol (1,3-dihydroxybenzene) by the denitrifying bacterium *Azoarcus anaerobius*. J Bacteriol 180:3644–3649.
14. Gorny N, Wahl G, Brune A, Schink B. 1992. A strictly anaerobic nitrate-reducing bacterium growing with resorcinol and other aromatic compounds. Arch Microbiol 158:48–53. https://doi.org/10.1007/BF00249065.
15. Gallus C, Gorny N, Ludwig W, Schink B. 1997. Anaerobic degradation of α-resorcylate by a nitrate-reducing bacterium, *Thauera aromatica* strain AR-1. Syst Appl Microbiol 20:540–544. https://doi.org/10.1016/S0723-2020(97)80023-9.
16. Philipp B, Schink B. 2000. Two distinct pathways for anaerobic degradation of aromatic compounds in the denitrifying bacterium *Thauera aromatica* strain AR-1. Arch Microbiol 173:91–96. https://doi.org/10.1007/s002039900112.
17. Philipp B, Kemmler D, Hellstern J, Gorny N, Caballero A, Schink B. 2002. Anaerobic degradation of protocatechuate (3,4-dihydroxybenzoate) by *Thauera aromatica* strain AR-1. FEMS Microbiol Lett 212:139–143. https://doi.org/10.1111/j.1574-6968.2002.tb11257.x.
18. Philipp B, Schink B. 2012. Different strategies in anaerobic biodegradation of aromatic compounds: nitrate reducers versus strict anaerobes. Environ Microbiol Rep 4:469–478. https://doi.org/10.1111/j.1758-2229.2011.00304.x.
19. Darley PI, Hellstern JA, Medina-Bellver JI, Marqués S, Schink B, Philipp B. 2007. Heterologous expression and identification of the genes involved in anaerobic degradation of 1,3-dihydroxybenzene (resorcinol) in *Azoarcus anaerobius*. J Bacteriol 189:3824–3833. https://doi.org/10.1128/JB.01729-06.
20. Molina-Fuentes A, Pacheco D, Marín P, Philipp B, Schink B, Marqués S. 2015. Identification of the gene cluster for the anaerobic degradation of 3,5-dihydroxybenzoate (alpha-resorcylate) in *Thauera aromatica* strain AR-1. Appl Environ Microbiol 81:7201–7214. https://doi.org/10.1128/AEM.01698-15.
21. Carmona M, Zamarro MT, Blazquez B, Durante-Rodriguez G, Juarez JF, Valderrama JA, Barragan MJL, Garcia JL, Diaz E. 2009. Anaerobic catabolism of aromatic compounds: a genetic and genomic view. Microbiol Mol Biol Rev 73:71–133. https://doi.org/10.1128/MMBR.00021-08.
22. Pacheco-Sánchez D, Molina-Fuentes A, Marín P, Medina-Bellver JI, González-López O, Marqués S. 2017. The *Azoarcus anaerobius* 1,3-dihydroxybenzene (resorcinol) anaerobic degradation pathway is controlled by the coordinated activity of two enhancer-binding proteins. Appl Environ Microbiol 83:e03042-16. https://doi.org/10.1128/AEM.03042-16.
23. Pareja E, Pareja-Tobes P, Manrique M, Pareja-Tobes E, Bonal J, Tobes R. 2006. ExtraTrain: a database of extragenic regions and transcriptional information in prokaryotic organisms. BMC Microbiol 6:29. https://doi.org/10.1186/1471-2180-6-29.
24. Momany C, Neidle EL. 2012. Defying stereotypes: the elusive search for a universal model of LysR-type regulation. Mol Microbiol 83:453–456. https://doi.org/10.1111/j.1365-2958.2011.07960.x.
25. Koentjoro MP, Adachi N, Senda M, Ogawa N, Senda T. 2018. Crystal structure of the DNA-binding domain of the LysR-type transcriptional regulator CbnR in complex with a DNA fragment of the recognition-binding site in the promoter region. FEBS J 285:977–989. https://doi.org/10.1111/febs.14380.
26. Rivas-Marin E, Floriano B, Santero E. 2016. Genetic dissection of independent and cooperative transcriptional activation by the LysR-type activator ThnR at close divergent promoters. Sci Rep 6:24538. https://doi.org/10.1038/srep24538.
27. Oliver P, Peralta-Gil M, Tabche ML, Merino E. 2016. Molecular and structural considerations of TF-DNA binding for the generation of biologically meaningful and accurate phylogenetic footprinting analysis: the LysR-type transcriptional regulator family as a study model. BMC Genomics 17:686. https://doi.org/10.1186/s12864-016-3025-3.

28. Maddocks SE, Oyston PC. 2008. Structure and function of the LysR-type transcriptional regulator (LTTR) family proteins. Microbiology 154:3609–3623. https://doi.org/10.1099/mic.0.2008/022772-0.
29. Lerche M, Dian C, Round A, Lönneborg R, Brzezinski P, Leonard GA. 2016. The solution configurations of inactive and activated DntR have implications for the sliding dimer mechanism of LysR transcription factors. Sci Rep 6:19988. https://doi.org/10.1038/srep19988.
30. Monferrer D, Tralau T, Kertesz MA, Dix I, Sola M, Uson I. 2010. Structural studies on the full-length LysR-type regulator TsaR from *Comamonas testosteroni* T-2 reveal a novel open conformation of the tetrameric LTTR fold. Mol Microbiol 75:1199–1214. https://doi.org/10.1111/j.1365-2958.2010.07043.x.
31. Porrúa O, García-Jaramillo M, Santero E, Govantes F. 2007. The LysR-type regulator AtzR binding site: DNA sequences involved in activation, repression and cyanuric acid-dependent repositioning. Mol Microbiol 66:410–427. https://doi.org/10.1111/j.1365-2958.2007.05927.x.
32. Härtig E, Frädrich C, Behringer M, Hartmann A, Neumann-Schaal M, Jahn D. 2018. Functional definition of the two effector binding sites, the oligomerization and DNA binding domains of the *Bacillus subtilis* LysR-type transcriptional regulator AlsR. Mol Microbiol 109:845–864. https://doi.org/10.1111/mmi.14089.
33. Bender RA. 2010. A NAC for regulating metabolism: the nitrogen assimilation control protein (NAC) from *Klebsiella pneumoniae*. J Bacteriol 192:4801–4811. https://doi.org/10.1128/JB.00266-10.
34. Breddermann H, Schnetz K. 2017. Activation of *leuO* by LrhA in *Escherichia coli*. Mol Microbiol 104:664–676. https://doi.org/10.1111/mmi.13656.
35. Nguyen Le Minh P, Velázquez Ruíz C, Vandermeeren S, Abwoyo P, Bervoets I, Charlier D. 2018. Differential protein-DNA contacts for activation and repression by ArgP, a LysR-type (LTTR) transcriptional regulator in *Escherichia coli*. Microbiol Res 206:141–158. https://doi.org/10.1016/j.micres.2017.10.009.
36. Reen FJ, Haynes JM, Mooij MJ, O'Gara F. 2013. A non-classical LysR-type transcriptional regulator PA2206 is required for an effective oxidative stress response in *Pseudomonas aeruginosa*. PLoS One 8:e54479. https://doi.org/10.1371/journal.pone.0054479.
37. Zhang WM, Zhang JJ, Jiang X, Chao HJ, Zhou NY. 2015. Transcriptional activation of multiple operons involved in *para*-nitrophenol degradation by *Pseudomonas* sp strain WBC-3. Appl Environ Microbiol 81:220–230. https://doi.org/10.1128/AEM.02720-14.
38. Frädrich C, March A, Fiege K, Hartmann A, Jahn D, Hartig E. 2012. The transcription factor AlsR binds and regulates the promoter of the alsSD operon responsible for acetoin formation in *Bacillus subtilis*. J Bacteriol 194:1100–1112. https://doi.org/10.1128/JB.06425-11.
39. Chen XC, Feng J, Hou BH, Li FQ, Li Q, Hong GF. 2005. Modulating DNA bending affects NodD-mediated transcriptional control in *Rhizobium leguminosarum*. Nucleic Acids Res 33:2540–2548. https://doi.org/10.1093/nar/gki537.
40. Spaink HP, Okker RJH, Wijffelman CA, Pees E, Lugtenberg BJJ. 1987. Promoters in the nodulation region of the *Rhizobium leguminosarum* sym plasmid pRL1JI. Plant Mol Biol 9:27–39. https://doi.org/10.1007/BF00017984.
41. MacLean AM, Anstey MI, Finan TM. 2008. Binding site determinants for the LysR-type transcriptional regulator PcaQ in the legume endosymbiont *Sinorhizobium meliloti*. J Bacteriol 190:1237–1246. https://doi.org/10.1128/JB.01456-07.
42. Kovacikova G, Skorupski K. 2002. Binding site requirements of the virulence gene regulator AphB: differential affinities for the *Vibrio cholerae* classical and El Tor *tcpPH* promoters. Mol Microbiol 44:533–547. https://doi.org/10.1046/j.1365-2958.2002.02914.x.
43. Tropel D, van der Meer JR. 2004. Bacterial transcriptional regulators for degradation pathways of aromatic compounds. Microbiol Mol Biol Rev 68:474–500. https://doi.org/10.1128/MMBR.68.3.474-500.2004.
44. Muraoka S, Okumura R, Ogawa N, Nonaka T, Miyashita K, Senda T. 2003. Crystal structure of a full-length LysR-type transcriptional regulator, CbnR: unusual combination of two subunit forms and molecular bases for causing and changing DNA bend. J Mol Biol 328:555–566. https://doi.org/10.1016/S0022-2836(03)00312-7.
45. Clark T, Haddad S, Neidle E, Momany C. 2004. Crystallization of the effector-binding domains of BenM and CatM, LysR-type transcriptional regulators from *Acinetobacter* sp. ADP1. Acta Crystallogr D Biol Crystallogr 60:105–108. https://doi.org/10.1107/S0907444903021589.
46. Zhou XH, Lou ZY, Fu S, Yang AQ, Shen HB, Li ZX, Feng YJ, Bartlam M, Wang HH, Rao ZH. 2010. Crystal structure of ArgP from *Mycobacterium tuberculosis* confirms two distinct conformations of full-length LysR transcriptional regulators and reveals its function in DNA binding and transcriptional regulation. J Mol Biol 396:1012–1024. https://doi.org/10.1016/j.jmb.2009.12.033.
47. Jo I, Chung IY, Bae HW, Kim JS, Song S, Cho YH, Ha NC. 2015. Structural details of the OxyR peroxide-sensing mechanism. Proc Natl Acad Sci U S A 112:6443–6448. https://doi.org/10.1073/pnas.1424495112.
48. López-Sánchez A, Rivas-Marín E, Martínez-Pérez O, Floriano B, Santero E. 2009. Co-ordinated regulation of two divergent promoters through higher-order complex formation by the LysR-type regulator ThnR. Mol Microbiol 73:1086–1100. https://doi.org/10.1111/j.1365-2958.2009.06834.x.
49. Sainsbury S, Lane LA, Ren J, Gilbert RJ, Saunders NJ, Robinson CV, Stuart DI, Owens RJ. 2009. The structure of CrgA from *Neisseria meningitidis* reveals a new octameric assembly state for LysR transcriptional regulators. Nucleic Acids Res 37:4545–4558. https://doi.org/10.1093/nar/gkp445.
50. Dominguez-Cuevas P, Marin P, Busby S, Ramos JL, Marques S. 2008. Roles of effectors in XylS-dependent transcription activation: intramolecular domain derepression and DNA binding. J Bacteriol 190:3118–3128. https://doi.org/10.1128/JB.01784-07.
51. Porrúa O, López-Sánchez A, Platero AI, Santero E, Shingler V, Govantes F. 2013. An A-tract at the AtzR binding site assists DNA binding, inducer-dependent repositioning and transcriptional activation of the PatzDEF promoter. Mol Microbiol 90:72–87. https://doi.org/10.1111/mmi.12346.
52. Stec E, Witkowska M, Hryniewicz MM, Brzozowski AM, Wilkinson AJ, Bujacz GD. 2004. Crystallization and preliminary crystallographic studies of the cofactor-binding domain of the LysR-type transcriptional regulator Cbl from *Escherichia coli*. Acta Crystallogr D Biol Crystallogr 60:1654–1657. https://doi.org/10.1107/S0907444904016841.
53. Ezezika OC, Haddad S, Neidle EL, Momany C. 2007. Oligomerization of BenM, a LysR-type transcriptional regulator: structural basis for the aggregation of proteins in this family. Acta Crystallogr F Struct Biol Cryst Commun 63:361–368. https://doi.org/10.1107/S1744309107019185.
54. Rosario CJ, Bender RA. 2005. Importance of tetramer formation by the nitrogen assimilation control protein for strong repression of glutamate dehydrogenase formation in *Klebsiella pneumoniae*. J Bacteriol 187:8291–8299. https://doi.org/10.1128/JB.187.24.8291-8299.2005.
55. Ausubel FM, Brent R, Kingston RE, Moore DD, Seidman JG, Smith JA, Struhl K. 1991. Current protocols in molecular biology. Wiley, New York, NY.
56. Miller J. 1972. Experiments in molecular genetics, p 352–355. Cold Spring Harbor Laboratory Press, Cold Spring Harbor, NY.
57. Aranda-Olmedo I, Ramos JL, Marques S. 2005. Integration of signals through Crc and PtsN in catabolite repression of *Pseudomonas putida* TOL plasmid pWW0. Appl Environ Microbiol 71:4191–4198. https://doi.org/10.1128/AEM.71.8.4191-4198.2005.
58. Kelley LA, Sternberg MJ. 2009. Protein structure prediction on the Web: a case study using the Phyre server. Nat Protoc 4:363–371. https://doi.org/10.1038/nprot.2009.2.
59. Boyer HW, Roulland-Dussoix D. 1969. A complementation analysis of the restriction and modification of DNA in *Escherichia coli*. J Mol Biol 41:459–472. https://doi.org/10.1016/0022-2836(69)90288-5.
60. De Lorenzo V, Herrero M, Jakubzik U, Timmis K. 1990. Mini-Tn*5* transposon derivatives for insertion mutagenesis, promoter probing, and chromosomal insertion of cloned DNA in Gram-negative eubacteria. J Bacteriol 172:6568–6572. https://doi.org/10.1128/jb.172.11.6568-6572.1990.
61. Sambrook J, Russell D. 2001. Molecular cloning: a laboratory manual, 3rd ed. Cold Spring Harbor Laboratory Press, Cold Spring Harbor, NY.
62. Casadaban MJ. 1976. Transposition and fusion of the lac genes to selected promoters in *Escherichia coli* using bacteriophage *lambda* and *Mu*. J Mol Biol 104:541–555. https://doi.org/10.1016/0022-2836(76)90119-4.
63. Kessler B, de Lorenzo V, Timmis KN. 1992. A general system to integrate *lacZ* fusions into the chromosomes of Gram-negative eubacteria: regulation of the Pm promoter of the TOL plasmid studied with all controlling elements in monocopy. Mol Gen Genet 233:293–301. https://doi.org/10.1007/BF00587591.
64. Kovach ME, Elzer PH, Hill DS, Robertson GT, Farris MA, Roop RM, II, Peterson KM. 1995. Four new derivatives of the broad-host-range cloning vector pBBR1MCS, carrying different antibiotic-resistance cassettes. Gene 166:175–176. https://doi.org/10.1016/0378-1119(95)00584-1.